SUPPLEMENTAL MATERIAL

MATERIALS AND METHODS

Yeast strains. The *gcd11:KanMX* strain J212 (*MATα leu2-3,-112 ura3-52 his3, gcd11Δ::KanMX* p[*GCD11*, *URA3*]) (6) was derived from the heterozygous *gcd11Δ::KanMX* diploid strain generated by the yeast genome deletion project and obtained from Research Genetics, Inc. (#20157). The diploid strain was transformed with the *URA3* plasmid pC2894 encoding *GCD11*, and then subjected to random spore analysis selecting for a Ura^+, Kan^r colony. Strain J212-1 was generated using plasmid shuffling to replace the [*GCD11*, *URA3*] plasmid in J212 with the [*GCD11*, *LEU2*] plasmid pC2887. To delete the *GCN2* gene in J212-1, the *loxP-URA3-loxP* cassette in the plasmid pUG72 was amplified by PCR using 5' and 3' primers with 45 bp complementarity to the sequences immediately preceding and following the *GCN2* ORF, respectively. The PCR product was introduced into strain J212-1 selecting for Ura^+ transformants. A segregant (J212-2) in which homologous recombination between the loxP sites eliminated the *URA3* marker (2) was obtained by selecting for growth on medium containing 5-fluoroorotic acid. Finally, the yeast strain J292 (*MATα leu2-3,-112 ura3-52 his3, gcn2Δ::loxP, gcd11Δ::KanMX* p[*GCD11*, *URA3*]) was generated by reintroducing the [*GCD11*, *URA3*] plasmid pC2895 and then screening for a Ura^+, Leu^- segregant following growth on rich medium. Deletion of the *GCN2* gene in the *pep4Δ* strain obtained from the yeast genome deletion collection was performed as described above generating the strain J293 (*MATα leu2Δ, ura3Δ, met15Δ, his3, pep4Δ::KanMX, gcn2Δ:loxP*.

Intragenic suppressor screening. The *GCD11* gene was amplified by PCR using the primers GCD11 PstI (5'-CTAGCTGCAGCAGATCCAACCGCGGGAAGTGGC-3') and GCD11 EcoRI (5'-ACGCGAATTCGTCTCCATGTACAAACCACCG-3'), and then inserted between the PstI and EcoRI sites of the vector pAlter Ex2 (Promega) creating the plasmid pC2857. Derivatives of p2857 containing the N135D or the N135A mutation were generated using the pAlter Ex2 mutagenesis kit and the oligos N135D (5'-AAATTTTAGCATTCGCGTAACCTAACTTAATAGTAATGTCACGTTCTAATTC-3') or N135A (5'-AAATTTTAGCATTCGCGTAACCTAACTTAATAGTAATGGCACGTTCTAATTC-3'), respectively. The *GCD11-N135D* and *GCD11-N135A* mutant alleles were transferred to the single copy-number *LEU2* vector YCplac111 creating the plasmids pC2858 and pC2859, respectively. The *GCD11-N135D* allele was also transferred to the single copy-number *URA3* vector YCplac33 creating pC2893. Plasmid pC2858 was subjected to random mutagenesis by passage through *E coli* mutator strain XL1-Red (Stratagene, Inc.). In initial screens the *GCD11-N135D* allele was readily converted to wild type when introduced into a strain carrying a wild type *GCD11* plasmid. To avoid this problem of gene conversion, the mutant library was introduced into a derivative of yeast strain J212 in which the wild type [*GCD11*, *URA3*] plasmid was replaced with the [*GCD11-N135D*, *URA3*] plasmid pC2893. Transformants were isolated, replica printed to 5-FOA medium to select for loss of the unmutated [*GCD11-N135D*, *URA3*] plasmid, and then colonies growing faster then the parent strain expressing *GCD11-N135D* were selected for further analysis. The *GCD11-N135D* plasmid was isolated from the faster growing colonies and re-tested in yeast to confirm that the suppressor phenotype was

associated with the plasmid. Finally, DNA sequencing of the suppressor plasmids identified the following suppressor alleles: T115A,N135D, pC2891; N135D,A208V, pC2889; N135D,A219T, pC2890; and N135D-A382V, pC2892.

Plasmids. Oligos SacI_5UTR (5'-CAGAGAGCTCCAGATCCAACCGCGGGAAGTGGC-3') + BamHI_His-tag (5'-AGCGGATCCGTGATGGTGATGGTGATGGTGATGTCCGGACATGTCTACCTCT AATGCGCGATGTTAAC-3') were used to amplify the *GCD11* gene from -500 to +1 (AUG start codon) for insertion of a His_8 tag between codons 2 and 3. The *His_8-GCD11* promoter fragment was cloned into the single copy-number *LEU2* vector YCplac111 and the high copy-number *LEU2* vector pRS425 generating the plasmids pC2860 and pC2861, respectively. Next, the *GCD11* ORF and ~ 430bp of the 3' flanking sequence was amplified by PCR using the oligos BamHI/GCD11 (5'CGCGGATCCGACTTACAAGACCAAGAACCTAGC-3') and SalI/GCD11 (5'-CGCAGTCGACTCTCCATGTACAAACCACCGATAAG-3'), and then cloned into the plasmids pC2860 and pC2861 between the BamHI and SalI sites to generate the low and high copy-number WT *His_8-GCD11* plasmids pC2872 and pC2873, respectively.

The A208V, A219T, or A382V mutation was introduced into the *GCD11* gene by fusion PCR using the outside primers BamHI/GCD11 and SalI/GCD11 and inner primers specific for each mutation as follows: A208V [(*A208V-NC*5'-GTAACGCAGCATCCATAACAGCTACACCTGATAACATAGTACTC -3') + (*A208V-cod* 5'-GAGTACTATGTTATCAGGTGTAGCTGTTATGGATGCTGCGTTAC-3'); A219T

[(*A219T_NC* 5'-GAGGTTGTGGACAAGATTCATTACCTGTAATCAACAGTAACGCAGCATC -3') and (*A219T_code* 5'- GATGCTGCGTTACTGTTGATTACAGGTAATGAATCTTGTCCACAACCTC -3')]; A382V [(*A382V_NC* 5'-GCAAACTTCAAGTCATTTTGTTCGACAAATAAGGAGACAATGTTAG-3') and (*A382V_code* 5'- CTAACATTGTCTCCTTATTTGTCGAACAAAATGACTTGAAGTTTGC -3')]. The PCR products were inserted between the BamHI and SalI sites of the plasmids pC2860 and pC2861 to generate the low and high copy-number *GCD11-T115A* (pC2868 and pC2869), *GCD11-A208V* (pC2862 and pC2863), *GCD11-A219T* (pC2866 and pC2867), and *GCD11-A382V* (pC2864 and pC2865) plasmids, respectively

The *GCD11-N135D* and *GCD11-N135A* alleles in the low copy-number *LEU2* plasmids pC2858 and pC2859, respectively, were amplified by PCR using the oligos BamHI/GCD11 and SalI/GCD11 and then subcloned between the BamHI and SalI sites of the plasmid pC2860 generating the *His_8-GCD11-N135D* and *His_8-GCD11-N135A* plasmids pC2874 and pC2875, respectively. The same PCR product carrying the *GCD11-N135D* sequences was subcloned to the plasmid pC2861 to generate the high copy-number *His_8-GCD11-N135D* plasmid pC2870.

To generate low and high copy-number His_8-tagged versions of the *GCD11* suppressor mutants, the suppressor alleles were amplified by PCR and cloned between the BamHI and SalI sites of the vectors pC2860 and pC2861, respectively. Plasmid pC2889 (*GCD11-N135D,A208V*) was used to create plasmids pC2876 (low copy, lc) and

pC2877 (high copy, hc); plasmid pC2890 (*GCD11-N135D,A219T*) was used to create plasmids pC2878 (lc) and pC2879 (hc); and plasmid pC2892 (*GCD11-N135D,A382V*) was used to create plasmids pC2880 (lc) and pC2881 (hc).

The *GCD11-N135A,382V* mutant was generated by fusion PCR using the *GCD11-N135A* plasmid pC2875 as a template and the oligos BamHI/GCD11 + *A382V_NC* (5'-GCAAACTTCAAGTCATTTTGTTCGACAAATAAGGAGACAATGTTAG-3') and SalI/GCD11 + *A382V_code* (5'- CTAACATTGTCTCCTTATTTGTCGAACAAAATGACTTGAAGTTTGC -3'). The PCR product was cloned between the BamHI and SalI sites of the vector pC2860 creating pC2884. The *GCD11-N135D-A382V-A219T* plasmid (pC3152) was generated by fusion PCR using pC2880 as a template and primers A219T_cod and A219T_NC (listed above) and cloned between the BamHI and Sal I sites of the plasmid pC2860.

The high copy number [*SUI2*, *SUI3*, *IMT4*] plasmid pC2887 was constructed in three steps. First, a SalI-BamHI *SUI3* fragment from the plasmid p920 was subcloned to pRS423 creating the plasmid pC2885. Next, the *IMT4* gene was amplified by PCR using the primers IMT4-SpeI (5'-TAACTAGTCGGAAGGTAAACTAACACGTAGG-3') and IMT4-SacII (5'-TCACCGCGGAACTATCAAGGGTCAGTCAATCAC-3'), and then subcloned between SpeI and SacII sites of pC2885 generating the plasmid pC2886. Finally, a BamHI fragment carrying the *SUI2* gene from the plasmid was inserted at the BamHI site of pC2886 to create pC2887. The chromosomal *SUI1* gene was amplified by PCR using the primers SacI-SUI1 (5`-AAACCGAGCTCGGTACCGCACATACTCCCGAATC-3`) and Xho-SUI1

(5`-CTGGATTCTCGAGAAGCTTGGGATTCCATGATTTC-3`) and then inserted between the SacI and XhoI sites of the high copy-number *HIS3* vector pRS423 to generate the plasmid pC2888.

Co-immunoprecipitation assay of eIF2 and ternary complex. Co-immunoprecipitation assays of eIF2 and Met-tRNA$_i^{Met}$ were performed as described previously (7) with modifications as described below. 100-ml cultures of yeast strains expressing WT eIF2γ, eIF2γ-N135D or eIF2γ-N135D,A208V were grown to OD_{600} = 0.9-1.0. Cells were harvested and suspended in 5 ml of buffer A [20 mM Tris-HCl (pH 7.5), 100 mM KCl, 5 mM $MgCl_2$, 0.1 mM EDTA, 7 mM β-mercaptoethanol, 5 mM NaF, 1 mM phenylmethylsulfonyl fluoride (PMSF), complete protease inhibitors (Roche), 1 µg/µl pepstain A and aprotinin]. Following addition of 0.5 ml glass beads, cells were broken by rapid mixing using a vortex mixer (10x by 30s) at 4 ˚C. One-third of the whole-cell extracts (WCEs) were set-aside as input samples and the remaining two-thirds of each WCE was mixed with 0.4 ml Ni^{2+}-agarose beads for 2 hr at 4 ˚C. Following washing, the beads were either mixed with SDS-sample buffer or suspended in 300 µl of 1x first-strand synthesis buffer (Life Technologies). Samples for Western analysis of eIF2 integrity were subjected to SDS-PAGE followed by immunoblotting with polyclonal antiserum against yeast eIF2α, eIF2β, and eIF2γ. For analysis of Met-tRNA$_i^{Met}$, RNA in the input and pull-down samples was extracted using citric acid-saturated phenol/chloroform/isoamyl alcohol (25:24:1). The extracted RNA was ethanol-precipitated, washed, dried briefly and suspended in 100 µl water.

Reverse transcription (RT)-PCR analysis of $tRNA_i^{Met}$ was performed as described previously (4) with modifications as described below.) For RT reactions (total volume 40 µl), 0.1- or 1.0-µl of RNA was incubated for 1 h at 42 ˚C with 200 ng random hexamers (Promega), 400 U of Superscript II reverse transcriptase and 1X First Strand Buffer (Life Technologies) 0.25 mM dithiothreitol, and 0.5 mM each nucleoside triphosphate. PCR reactions contained 80 pmol primers (5' primer: 5'-CAGGGCTCATAACCCTGAT-3' and 3' primer: 5'-TGGTAGCGCCGCTCGGTTTC-3' to give 50-bp product), either 0.2 or 1 µl RT products, and 0.5X PureTaq PCR Beads (GE Healthcare) in a total volume of 14 µl. PCR was performed under the following conditions: (1) 95 ˚C for 2 min, (2) 30 cycles of 95 ˚C for 1 min, 55 ˚C for 30s, 72 ˚C for 1 min, and (3) 72 ˚C for 3 min. Reaction products were resolved by electrophoresis on a 20% TBE-acrylamide gel (Invitrogen), and stained with ethidium bromide. Gels were scanned and quantified using ImageJ software (NIH).

In vivo 43S complex formation. Formaldehyde cross-linking and fractionation of extracts by sedimentation through sucrose density gradients were performed as described previously (5). WT or eIF2γ-N135D mutant strains were cultured in 300 ml minimal medium plus appropriate supplements to OD_{600}~1.5. The cultures were cross-linked with 2% HCHO in an ice-cold bottle and incubated on ice for 1 h with occasional gentle shaking. The cross-linking reaction was stopped by the addition of 100 mM glycine and the harvested cells were stored at -70 ˚C. The cross-linked cells were broken with glass beads and equal amounts of WCEs (A_{260} = 28) were separated by sedimentation through 7.5-30% sucrose gradients using an SW41 rotor (Beckmen) at 41000 rpm for 4.45 h. The

gradients were fractionated into 700 µl fractions, and 35 µl aliquots were mixed with 6X loading dye [300 mM Tris-HCl pH 6.8, 12% (w/v) SDS, 0.6% (w/v) bromophenol blue, 60% (v/v) glycerol and 600 mM β-mercaptoethanol] and separated on 4-12% NuPAGE gels (Invitrogen). Immunoblot analysis was performed using polyclonal antiserum against yeast eIF2α, eIF2γ, eIF1, eIF3a and the 40S ribosomal subunit protein S4.

SUPPLEMENTARY FIGURES

Figure S1. Analysis of eIF2 integrity and ternary complexes in whole cell extracts. **(A)** Co-precipitation of eIF2α and eIF2β with eIF2γ from crude cell extracts. WCEs were prepared from strains expressing the indicated WT or mutant forms of His-tagged eIF2γ and mixed with Ni^{2+}-agarose beads. Pellet fractions were analyzed by SDS-PAGE and immunoblot analysis using anti-eIF2γ (top), anti-eIF2β (middle), and anti-eIF2α (bottom) antiserum. **(B)** Co-precipitation of $tRNA_i^{Met}$ with eIF2 from crude cell extracts. $tRNA_i^{Met}$ in pellet fractions described in panel A was detected by RT-PCR analysis as described in Materials and Methods. Inputs represent 3% of the starting material and the two lanes represent 0.1 and 1.0X of each sample. Presented at the top of the co-immunoprecipitation (Co-IP) lanes is the amount of $tRNA_i^{Met}$ co-immunoprecipitated with the eIF2γ mutants – values were normalized to the amount recovered with WT eIF2γ.

Figure S2. Analysis of growth of yeast strains overexpressing eIF2γ mutants. Derivatives of yeast strain J292 expressing the indicated WT or mutant forms of eIF2γ

from low (left panel) or high (right panel) copy-number plasmids were serially diluted, spotted on SD medium, and incubated 3 days at 30 ˚C as described in Figure 1B.

Figure S3. Determination of equilibrium dissociation constants for GDP binding to eIF2 complexes containing WT or mutant forms of eIF2γ. 40 nM purified WT or indicated eIF2 mutant complexes were incubated with 0-400 nM [^{3}H]GDP in 30 µl reaction volume at 26 ˚C for 10 min. Nitrocellulose filter binding assays were performed as described previously (3), and the data were plotted using Sigma Plot 9.0 software. Each point represents the mean of at least three independent experiments, and error bars were removed to simplify viewing of the results. The dissociation constants (K_d) in nM are summarized in Table 1.

Figure S4. Determination of equilibrium dissociation constants for GTP binding to eIF2 complexes containing WT or mutant forms of eIF2γ. 40 nM purified WT or indicated eIF2 mutant complexes were incubated with 0-10 µM [^{3}H]GTP in 30 µl reaction volume at 26 ˚C for 10 min. Nitrocellulose filter binding assays were performed as described previously (3), and the data was plotted using Sigma Plot 9.0 software. Each point represents the mean of at least three independent experiments, and error bars were removed to simplify viewing of the results. The dissociation constants (K_d) in µM are summarized in Table 1.

Figure S5. Determination of the equilibrium dissociation constants for Met-tRNA$_i^{Met}$ binding to eIF2 complexes containing WT or mutant forms of eIF2γ. 1 nM

[^{3}H]Met-tRNA$_i^{Met}$ was incubated with 0-300 nM purified WT or indicated eIF2 mutant complexes in 30 µl reaction volume at 26 ˚C for 10 min. Nitrocellulose filter binding assays were performed as described previously (3), and the data was plotted using Sigma Plot 9.0 software. Each point represents the mean of at least three independent experiments, and error bars were removed to simplify viewing of the results. The dissociation constants (K_d) in nM are summarized in Table 1.

Figure S6. Rate of GTP hydrolysis by eIF2 complexes containing WT or mutant forms of eIF2γ. The experiment was performed as described in Alone et al (1). Preformed eIF2•GTP•Met-tRNA$_i^{Met}$ ternary complexes containing 40 pmoles [γ-^{33}P]GTP were mixed with preformed 40S complexes (40S subunits plus eIF1, eIF1A, eIF5 and model mRNA), and the fraction GTP hydrolyzed at each time point was monitored by thin layer chromatography as previously described (1). The data were plotted using Sigma Plot 9.0 software, and each data point represents the mean of at least three independent experiments. The error bars were removed to simplify viewing of the results. The rate of GTP hydrolysis and the V_{max} for the reactions are summarized in Table 1.

Figure S7. Analysis of eIF1 binding to 40S complexes in HCHO-treated cells. (A) WT or eIF2γ-N135D mutant strains were grown in minimal medium and cross-linked with 2% HCHO (final concentration) for 1 hr at 4 ˚C. WCEs were separated on 7.5-30% sucrose gradients, and gradient fractions were subjected to Western analysis using antiserum directed against the indicated proteins. The first lane contains 8% of the input from the WCE. Fractions containing 40S subunits are boxed. **(B)** Initiation factor binding

to 40S subunits in three replicates of the experiment in (A) were quantified relative to the 40S protein S4. Results are means +/- s.e. (n = 3).

REFERENCES

1. **Alone, P. V., and T. E. Dever.** 2006. Direct binding of translation initiation factor eIF2γ-G domain to its GTPase-activating and GDP-GTP exchange factors eIF5 and eIF2Bε. J Biol Chem **281:**12636-44.
2. **Gueldener, U., J. Heinisch, G. J. Koehler, D. Voss, and J. H. Hegemann.** 2002. A second set of loxP marker cassettes for Cre-mediated multiple gene knockouts in budding yeast. Nucleic Acids Res **30:**e23.
3. **Kapp, L. D., and J. R. Lorsch.** 2004. GTP-dependent recognition of the methionine moiety on initiator tRNA by translation factor eIF2. J Mol Biol **335:**923-36.
4. **Larminie, C. G., J. E. Sutcliffe, K. Tosh, A. G. Winter, Z. A. Felton-Edkins, and R. J. White.** 1999. Activation of RNA polymerase III transcription in cells transformed by simian virus 40. Mol Cell Biol **19:**4927-4934.
5. **Nielsen, K., B. Szamecz, L. Valasek, A. Jivotovskaya, B. S. Shin, and A. G. Hinnebusch.** 2004. Functions of eIF3 downstream of 48S assembly impact AUG recognition and *GCN4* translational control. EMBO J **23:**1166-1177.
6. **Roll-Mecak, A., P. Alone, C. Cao, T. E. Dever, and S. K. Burley.** 2004. X-ray structure of translation initiation factor eIF2γ: implications for tRNA and eIF2α binding. J Biol Chem **279:**10634-42.

7. **Singh, C. R., T. Udagawa, B. Lee, S. Wassink, H. He, Y. Yamamoto, J. T. Anderson, G. D. Pavitt, and K. Asano.** 2007. Change in nutritional status modulates the abundance of critical pre-initiation intermediate complexes during translation initiation in vivo. J Mol Biol **370:**315-330.

A

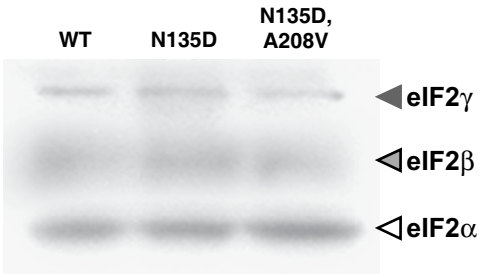

B

	100%		36%		75%
WT Input	WT Co-IP	N135D Input	N135D Co-IP	N135D, A208V Input	N135D, A208V Co-IP

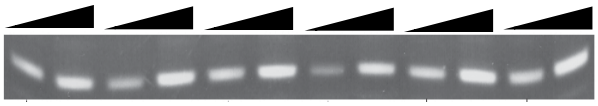

S1

S2

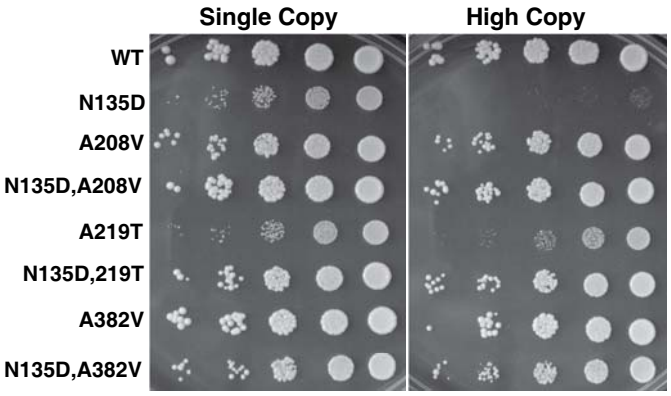
Single Copy
High Copy
WT
N135D
A208V
N135D,A208V
A219T
N135D,219T
A382V
N135D,A382V

S3

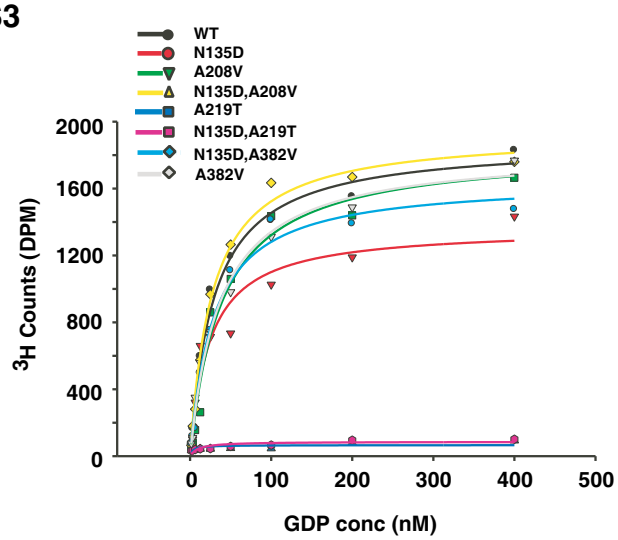
WT
N135D
A208V
N135D,A208V
A219T
N135D,A219T
N135D,A382V
A382V
3H Counts (DPM)
GDP conc (nM)

S4

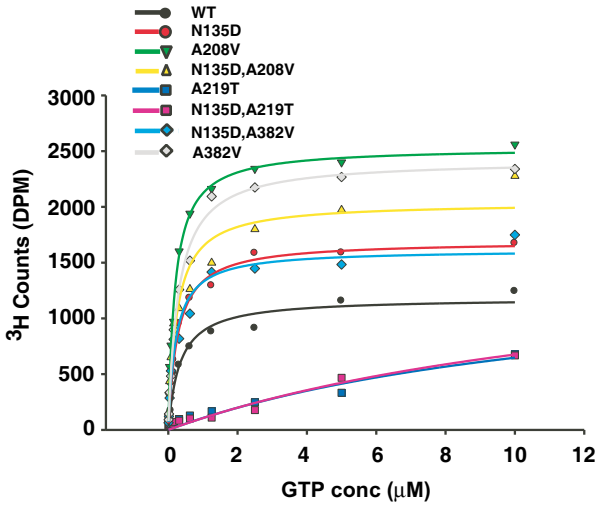
WT
N135D
A208V
N135D,A208V
A219T
N135D,A219T
N135D,A382V
A382V
3H Counts (DPM)
GTP conc (μM)

S5

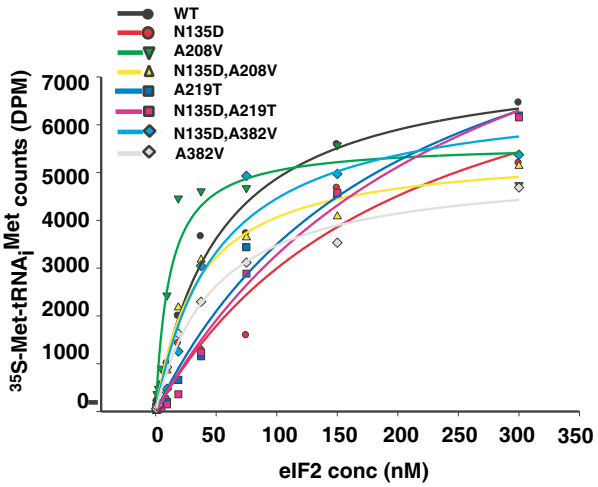
WT
N135D
A208V
N135D,A208V
A219T
N135D,A219T
N135D,A382V
A382V
35S-Met-tRNAiMet counts (DPM)
eIF2 conc (nM)

S6

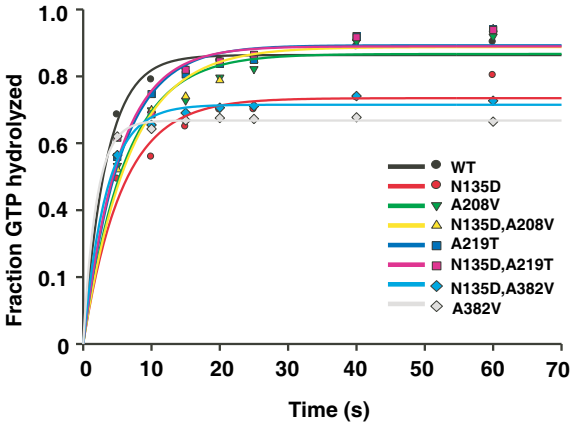
Fraction GTP hydrolyzed
Time (s)
WT
N135D
A208V
N135D,A208V
A219T
N135D,A219T
N135D,A382V
A382V

A

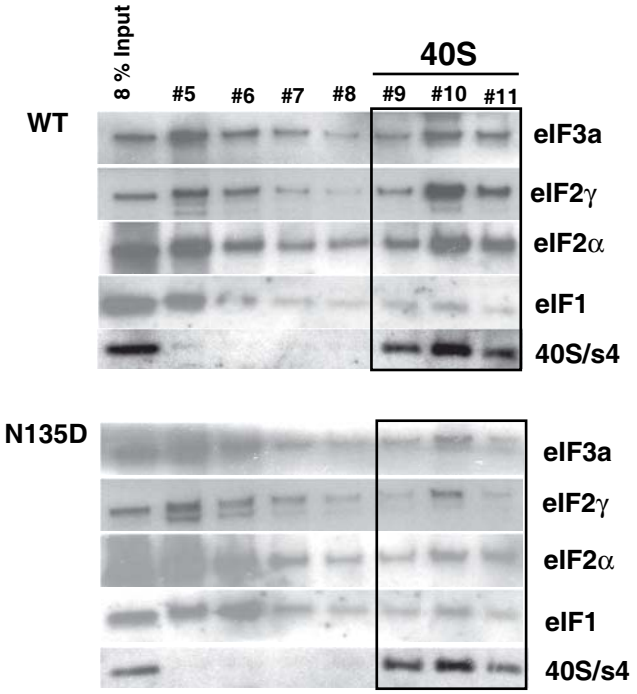
8 % Input
40S
#5
#6
#7
#8
#9
#10
#11
WT
eIF3a
eIF2γ
eIF2α
eIF1
40S/s4
N135D
eIF3a
eIF2γ
eIF2α
eIF1
40S/s4

B

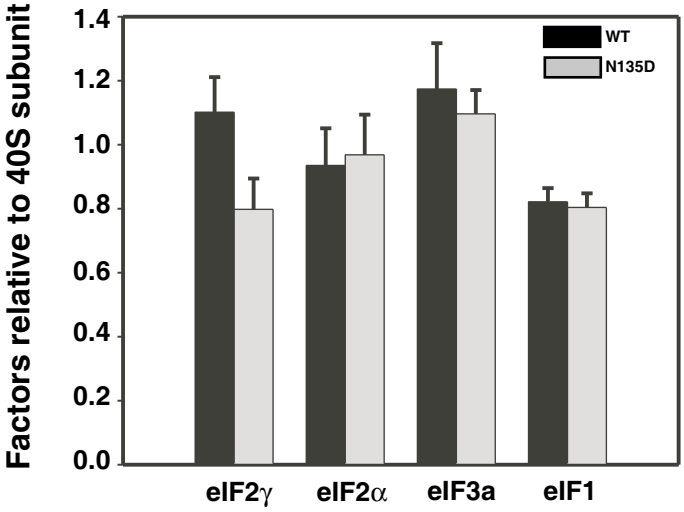
Factors relative to 40S subunit
1.4
1.2
1.0
0.8
0.6
0.4
0.2
0.0
WT
N135D
eIF2γ
eIF2α
eIF3a
eIF1